Adaptive trajectory tracking control of space manipulator with fast fixed-time convergence

Yuxin Yan[a*], Hutao Cui[a] and Peng Han[b]
[a] Deep Space Exploration Research Centre, Harbin Institute of Technology University, China;
[b]School of Civil Engineering, Harbin Institute of Technology University, China

ABSTRACT

This paper investigates the problem of fixed-time tracking control for a space manipulator subject to internal uncertainties and unknown disturbances. To shorten the system's response time, a novel globally fast fixed-time stable system is first developed. Based on this system, a novel non-singular terminal sliding mode surface is designed, which ensures fast and fixed-time convergence regardless of the initial states. A robust fast fixed-time sliding mode controller is then constructed by combining an adaptive mechanism, which can guarantee the tracking errors converge quickly to small regions around the origin within a bounded time. With the proposed control method, there is no required to know prior information about the bound of the lumped uncertainty. The suggested scheme is analysed using the Lyapunov stability theory, and the effectiveness is demonstrated through numerical simulations.

Keywords: Space manipulator, trajectory tracking, fixed-time control.

1. INTRODUCTION

Recently, the application of space manipulators (SMs) in deep space exploration has received widespread attention[1]. Compared to traditional ground-based manipulators, it's more challenging to design tracking controllers for SMs due to its highly coupled characteristic. Moreover, unknown disturbances and parameter uncertainties are inevitable problems for SMs, which can further damage the control system performance and even destabilise the whole system.

Even with different tracking control techniques, including neural network (NN)[4], backstepping control[3], sliding mode control (SMC)[2], etc., the system's asymptotic convergence is only guaranteed. The idea of finite-time stabilisation was subsequently put out by[5], allowing for successful trajectory tracking within a finite time. However, the disadvantage of the finite-time stability-based controllers is that the stabilisation time is sensitive to system's beginning states. To solve this issue, control schemes based upon fixed-time stability was put forward[6, 7], which results in the fixed-time convergence independent of initial state. Noteworthy, the majority of existing fixed-time controls suffer from the problem of converging not fast enough.

Inspired by the above discussions, a robust fixed-time sliding mode controller is developed for a space manipulator by combining a novel fast fixed-time stable theorem and adaptive technique. With the help of this method, it enables estimate the lumped uncertainties' upper bound effectively and realize the fixed-time convergence of trajectory error.

2. PROBLEM STATEMENT

Considering the disturbances, the free-floating SM model is expressed as follows[8]:

$$\mathbf{H}(\mathbf{q})\ddot{\mathbf{q}} + \mathbf{C}(\mathbf{q},\dot{\mathbf{q}})\dot{\mathbf{q}} = \boldsymbol{\tau} + \mathbf{d} \tag{1}$$

The states $\mathbf{q}$, $\dot{\mathbf{q}}$, $\ddot{\mathbf{q}} \in \mathbb{R}^n$ refer to the joint position, velocity, and acceleration vectors, respectively. $\mathbf{C}(\mathbf{q},\dot{\mathbf{q}}) = \mathbf{C}_0(\mathbf{q},\dot{\mathbf{q}}) + \Delta\mathbf{C}(\mathbf{q},\dot{\mathbf{q}})$ denotes the Coriolis and Centrifugal matrix and $\mathbf{H}(\mathbf{q}) = \mathbf{H}_0(\mathbf{q}) + \Delta\mathbf{H}(\mathbf{q})$ denotes the inertia matrix, where $\mathbf{C}_0(\mathbf{q},\dot{\mathbf{q}})$, $\mathbf{H}_0(\mathbf{q})$ represent the nominal item, and $\Delta\mathbf{C}_0(\mathbf{q},\dot{\mathbf{q}})$, $\Delta\mathbf{H}(\mathbf{q})$ represent the uncertainty.

[*] hityyx110119@126.com

International Conference on Optics, Electronics, and Communication Engineering (OECE 2024),
edited by Yang Yue, Proc. of SPIE Vol. 13395, 133950U · © 2024 SPIE · 0277-786X · Published

doi: 10.1117/12.3049873

Regarding $\mathbf{e}_1 = \mathbf{q} - \mathbf{q}_d$ and $\mathbf{e}_2 = \dot{\mathbf{q}} - \dot{\mathbf{q}}_d$ as the position tracking error and its time derivative with the desired position $\mathbf{q}_d \in \mathbb{R}^n$ and its derivative $\dot{\mathbf{q}}_d \in \mathbb{R}^n$. From (1), one can obtain the corresponding equation of the tracking error:

$$\begin{cases} \dot{\mathbf{e}}_1 = \mathbf{e}_2 \\ \dot{\mathbf{e}}_2 = \mathbf{H}_0^{-1}(\mathbf{q})\boldsymbol{\tau} - \mathbf{H}_0^{-1}(\mathbf{q})\mathbf{C}_0(\mathbf{q},\dot{\mathbf{q}})\dot{\mathbf{q}} + \mathbf{f}_{dis} - \ddot{\mathbf{q}}_d \end{cases} \tag{2}$$

Where $\mathbf{f}_{dis} = \mathbf{H}_0^{-1}(\mathbf{q})\left(\mathbf{d} - \Delta\mathbf{C}(\mathbf{q},\dot{\mathbf{q}})\dot{\mathbf{q}} - \Delta\mathbf{H}\left(\mathbf{q}\right)\ddot{\mathbf{q}}\right)$ represents the lumped uncertainty. According to the property of the inertia matrix, the non-singularity of $\mathbf{H}_0^{-1}$ is always guaranteed.

Assumption 1[9]. Suppose that $\mathbf{f}_{dis}$ is bounded, satisfying $\left\|\mathbf{f}_{dis}\right\| \le c_1 + c_2\left\|\mathbf{q}\right\| + c_3\left\|\dot{\mathbf{q}}\right\|^2 = \mathbf{c}_d^T\boldsymbol{\theta}$ with three constants $c_1, c_2, c_3 > 0$.

3. CONTROLLER DESIGN

3.1 Novel fast fixed-time stable system

Theorem 1: Define a system as

$$\dot{y} = -N(y)(k_1\mathbf{sig}^{1+\sigma}(y) + k_2\mathbf{sig}^{\lambda}(y)) \tag{3}$$

Where $N(y) = 1 + 2s_1\arctan(s_2\,|\,y\,|^{s_3})/\pi$ with three positive constants $s_1 > 0$, $s_2 > 0$, $s_3 > 0$. $\sigma = \dfrac{\alpha(1+\mathrm{sgn}(|\,y\,|-1))}{2} + \dfrac{(\beta-1)(1-\mathrm{sgn}(|\,y\,|-1))}{2}$, $\lambda = \dfrac{(2\beta+\alpha)}{2} + \dfrac{(2-2\beta+\alpha)\mathrm{sgn}(|\,y\,|-1)}{2}$ with two constants α, β satisfying $\alpha > 1$ and $1/2 < \beta < 1$. $k_1 > 0$ and $k_2 > 0$ are two scalars. Then, system (3) is fixed-time stable. *Proof*: Let $z = |\,y\,|^{1-\beta}$ and its time derivative is calculated as

$$\begin{aligned} \dot{z} &= (1-\beta)\mathbf{sig}^{-\beta}(y)\dot{y} \\ &= -(1-\beta)N(y)(k_1\,|\,y\,|^{1+\sigma-\beta} + k_2\,|\,y\,|^{\lambda-\beta}) \\ &= -(1-\beta)N(y)(k_1\,|\,z\,|^{\varepsilon} + k_2\,|\,z\,|^{\gamma}) \end{aligned} \tag{4}$$

where $\varepsilon = 1 + \dfrac{\sigma}{1-\beta}$ and $\gamma = \dfrac{\lambda-\beta}{1-\beta}$.

Solving (4), the settling time T_1 is given by

$$\begin{aligned} T_1 &= \frac{1}{1-\beta}\int_0^{z(0)} \frac{dz}{N(y)(k_1\,|\,z\,|^{\varepsilon} + k_2\,|\,z\,|^{\gamma})} \\ &= \frac{1}{1-\beta}\left(\int_0^1 \frac{dz}{N(y)(k_1 + k_2\,|\,z\,|^{-1})} + \int_1^{z(0)} \frac{dz}{N(y)(k_1+k_2)\,|\,z\,|^{\rho}}\right) \\ &\le \frac{1}{1-\beta}\left\{\frac{1}{k_1}\left(1 - \frac{k_2}{k_1}\ln\left(1+\frac{k_1}{k_2}\right)\right) + \frac{1-z(0)^{1-\rho}}{(k_1+k_2)(\rho-1)}\right\} \end{aligned} \tag{5}$$

Invoking $\rho = 1 + \dfrac{\alpha}{(1-\beta)} > 1$ and $z(0) > 0$, the convergence time T_1 is obtained as

$$T_1 \le \frac{1}{(1-\beta)k_1}\left(1 - \frac{k_2}{k_1}\ln\left(1+\frac{k_1}{k_2}\right)\right) + \frac{1}{\alpha(k_1+k_2)} \tag{6}$$

This completes the proof.

Remark 1. As (6) demonstrates, the upper bound of T_1 depends only on the system parameters k_1, k_2, α, β regardless of any system initial states.

Remark 2. Ni et.al[10] [10] developed a fast fixed-time stable system $\dot{y} = -k_1 y^{1/2+\alpha/2+(\alpha-1)\mathrm{sgn}(|y|-1)/2} - k_2 y^{\beta}$ with the upper bound on stabilization time $\frac{1}{k_1(1-\beta)}\ln(1+\frac{k_1}{k_2}) + \frac{1}{k_1(\alpha-1)}$. Cao et.al[11] constructed another fast fixed-time stable system $\dot{y} = -k_1 y^{1+\alpha(1+\mathrm{sgn}(|y|-1))/2} - k_2 y^{\beta}$ with the upper bound on stabilization time $\frac{1}{k_1(1-\beta)}\ln(1+\frac{k_1}{k_2}) + \frac{1}{k_1\alpha}$. Through comparison, the proposed stable system (3) is found to respond more quickly than two existing systems.

3.2 Sliding mode surface design

According to **Theorem 1** and switching method in[12], a novel non-singular fast sliding mode surface (NFSMS) is developed as

$$\mathbf{s} = \mathbf{e}_2 + N(\mathbf{e}_1)\left(k_a\mathbf{S}_c + k_b\mathbf{S}_z\right) \tag{7}$$

where $k_a > 0$ and $k_b > 0$ are two scalars, $N(\mathbf{e}_1) = 1 + \frac{2}{\pi} s_m \arctan(s_n \|\mathbf{e}_1\|^{s_r})$ and constants $s_m > 0, s_n > 0, s_r > 0$. The i th elements of $\mathbf{S}_c$ and $\mathbf{S}_z$ can be denoted as s_{ci} and s_{zi}, respectively, and have the following forms

$$S_{ci} = \begin{cases} \mathrm{sig}^{1+2\sigma_1}(e_{1i}) & \text{if} \quad \bar{s}_i = 0 \quad \text{or} \quad \bar{s}_i \neq 0, |e_{1i}| \geq \delta \\ l_1 e_{1i} + l_2 e_{1i}^2 \mathrm{sgn}(e_{1i}) + l_3 e_{1i}{}^3 & \text{if} \quad \bar{s}_i \neq 0, |e_{1i}| < \delta \end{cases} \tag{8}$$

$$S_{zi} = \begin{cases} \mathrm{sig}^{2\lambda_1 - 1}(e_{1i}) & \text{if} \quad \bar{s}_i = 0 \quad \text{or} \quad \bar{s}_i \neq 0, |e_{1i}| \geq \delta \\ g_1 e_{1i} + g_2 e_{1i}^2 \mathrm{sgn}(e_{1i}) + g_3 e_{1i}{}^3 & \text{if} \quad \bar{s}_i \neq 0, |e_{1i}| < \delta \end{cases} \tag{9}$$

where $i = 1, 2, \ldots, n$, $0 < \delta < 1$ is a constant, $\sigma_1 = \alpha_1(1+\mathrm{sgn}(\|\mathbf{e}_1\|-1))/2 + (\beta_1 - 1)(1-\mathrm{sgn}(\|\mathbf{e}_1\|-1))/2$, $\lambda_1 = (2\beta_1 + \alpha_1)/2 + (2 - 2\beta_1 + \alpha_1)\mathrm{sgn}(\|\mathbf{e}_1\|-1)/2$ with two constants α_1, β_1 satisfying $\alpha_1 > 1$, $3/4 < \beta_1 < 1$. To make the functions S_{ci} and S_{zi}, and their time derivative continuous, the values of l_1, l_2, l_3, g_1, g_2, g_3 are chosen as

$$l_1 = (2\beta_1 - 3)(\beta_1 - 2)\delta^{2\beta_1 - 2} \tag{10}$$

$$l_2 = -(2\beta_1 - 2)(2\beta_1 - 4)\delta^{2\beta_1 - 3} \tag{11}$$

$$l_3 = (\beta_1 - 1)(2\beta_1 - 3)\delta^{2\beta_1 - 4} \tag{12}$$

$$g_1 = (4\beta_1 - 5)(2\beta_1 - 3)\delta^{4\beta_1 - 4} \tag{13}$$

$$g_2 = -(4\beta_1 - 4)(4\beta_1 - 6)\delta^{4\beta_1 - 5} \tag{14}$$

$$g_3 = (2\beta_1 - 2)(4\beta_1 - 5)\delta^{4\beta_1 - 6} \tag{15}$$

$$\bar{\mathbf{s}} = \mathbf{e}_2 + N(\mathbf{e}_1)(k_a \mathbf{sig}^{1+2\sigma_1}(\mathbf{e}_1) + k_b \mathbf{sig}^{2\lambda_1 - 1}(\mathbf{e}_1)) \tag{16}$$

3.3 Trajectory Tracking Control Law Design

Using the error equation (2), the time derivate of the NFSMS (7) can be given by

$$\begin{aligned} \dot{\mathbf{s}} &= \dot{\mathbf{e}}_2 + N(\mathbf{e}_1)\left(k_a\dot{\mathbf{S}}_c + k_b\dot{\mathbf{S}}_z\right) + \dot{N}(\mathbf{e}_1)\left(k_a\mathbf{S}_c + k_b\mathbf{S}_z\right) \\ &= \mathbf{H}_0^{-1}(\mathbf{q})\boldsymbol{\tau} - \mathbf{H}_0^{-1}(\mathbf{q})\mathbf{C}_0(\mathbf{q},\dot{\mathbf{q}})\dot{\mathbf{q}} + \mathbf{f}_{dis} - \ddot{\mathbf{q}}_d \\ &\quad + N(\mathbf{e}_1)\left(k_a\dot{\mathbf{S}}_c + k_b\dot{\mathbf{S}}_z\right) + \dot{N}(\mathbf{e}_1)\left(k_a\mathbf{S}_c + k_b\mathbf{S}_z\right) \end{aligned} \tag{17}$$

where the i th element of $\dot{S}_c$ and $\dot{S}_z$ are given by

$$\dot{S}_{ci} = \begin{cases} (1+2\sigma_1)|e_{1i}|^{2\sigma_1} e_{2i} & \text{if} \quad \bar{s}_i = 0 \quad \text{or} \quad \bar{s}_i \neq 0, |e_{1i}| \geq \delta \\ l_1 e_{2i} + 2l_2|e_{1i}|e_{2i} + 3l_3 e_{1i}{}^2 e_{2i} & \text{if} \quad \bar{s}_i \neq 0, |e_{1i}| < \delta \end{cases} \tag{18}$$

$$\dot{S}_{zi}=\begin{cases}(2\lambda_1-1)\left|e_{1i}\right|^{2\lambda_1-2}\mathrm{e}_{2i} & \text{if}\quad \overline{s_i}=0\quad \text{or}\quad \overline{s_i}\neq 0,|\,\mathrm{e}_{1i}\,|\geq\delta\\ g_1e_{2i}+2g_2\left|e_{1i}\right|e_{2i}+3g_3e_{1i}{}^2e_{2i} & \text{if}\quad \overline{s_i}\neq 0,|\,\mathrm{e}_{1i}\,|<\delta\end{cases}\tag{19}$$

To obtain high-precision trajectory tracking, a robust fast fixed-time controller is developed as follows

$$\boldsymbol{\tau}=\mathbf{u}_{eq}+\mathbf{u}_{sw}+\mathbf{u}_{ad}\tag{20}$$

$$\mathbf{u}_{eq}=-\mathbf{H}_0(\mathbf{q})\left(-\mathbf{H}_0^{-1}(\mathbf{q})\mathbf{C}_0(\mathbf{q},\dot{\mathbf{q}})\dot{\mathbf{q}}-\ddot{\mathbf{q}}_d+N(\mathbf{e}_1)\left(k_a\dot{\mathbf{S}}_c+k_b\dot{\mathbf{S}}_z\right)+\dot{N}(\mathbf{e}_1)\left(k_a\mathbf{S}_c+k_b\mathbf{S}_z\right)\right)\tag{21}$$

$$\mathbf{u}_{sw}=-\mathbf{H}_0(\mathbf{q})N(\mathbf{s})(\gamma_1\mathbf{sig}^{1+2\sigma_2}(\mathbf{s})+\gamma_2\mathbf{sig}^{2\lambda_2-1}(\mathbf{s})+\gamma_3\mathbf{s})\tag{22}$$

$$\mathbf{u}_{ad}=-\mathbf{H}_0(\mathbf{x}_1)\frac{\hat{\mathbf{c}}_m^T\boldsymbol{\Theta}}{2\varepsilon_N^2}\mathbf{s}\tag{23}$$

where $\sigma_2=\frac{\alpha_2}{2}(1+\mathrm{sgn}(\left\|\mathbf{e_1}\right\|-1))+(\frac{\beta_2}{2}-\frac{1}{2})(1-\mathrm{sgn}(\left\|\mathbf{e_1}\right\|-1))$, $\lambda_2=(\beta_2+\frac{\alpha_2}{2})+(1-\beta_2+\frac{\alpha_2}{2})\mathrm{sgn}(\left\|\mathbf{e_1}\right\|-1)$ with $\alpha_2>1$, $\frac{1}{2}<\beta_2<1$. γ_1, γ_2, γ_3 are positive design parameters, $N(\mathbf{s})=1+2ss_m\arctan(ss_n\left\|\mathbf{s}\right\|^{ss_r})/\pi$ with ss_m, ss_n and $ss_r>0$, $\hat{\mathbf{c}}_m$ stands for the estimate of $\mathbf{c}_m=[c_1^2,c_2^2,c_3^2]^T$, and $\boldsymbol{\Theta}=[1,\left\|\mathbf{x}_1\right\|^2,\left\|\mathbf{x}_1\right\|^4]^T$. Introducing the following adaptive update law:

$$\dot{\hat{\mathbf{c}}}_m=\boldsymbol{\eta}\left(\frac{\boldsymbol{\Theta}\left\|\mathbf{s}\right\|^2}{2\varepsilon_N^2}-\boldsymbol{\upsilon}\hat{\mathbf{c}}_m\right)\tag{24}$$

where the constant $\varepsilon_N>0$, $\boldsymbol{\eta}=diag(\eta_1,\eta_2,\eta_3)$ and $\boldsymbol{\upsilon}=diag(\nu_1,\nu_2,\nu_3)$ denote two positive matrices.

3.4 Stability analysis

Theorem 3: The closed-loop system is practically fixed-time stable when the fixed-time tracking controller (20)-(23) is implemented to the SM system (2) with the adaptive update law (24).
Proof: Let a Lyapunov function

$$V_2=\frac{1}{2}\mathbf{s}^T\mathbf{s}+\frac{1}{2}\tilde{\mathbf{c}}_m^T\boldsymbol{\eta}^{-1}\tilde{\mathbf{c}}_m\tag{25}$$

where $\tilde{\mathbf{c}}_m=\mathbf{c}_m-\hat{\mathbf{c}}_m$. The time derivative of V_2 yields

$$\begin{aligned}\dot{V}_2&=\mathbf{s}^T\dot{\mathbf{s}}-\tilde{\mathbf{c}}_m^T\boldsymbol{\eta}^{-1}\dot{\hat{\mathbf{c}}}_m\\&=-\mathbf{s}^TN(\mathbf{s})(\gamma_1\mathbf{sig}^{1+2\sigma_2}(\mathbf{s})+\gamma_2\mathbf{sig}^{2\lambda_2-1}(\mathbf{s})+\gamma_3\mathbf{s})+\mathbf{s}^T\mathbf{f}_{dis}-\mathbf{s}^T\frac{\hat{\mathbf{c}}_m^T\boldsymbol{\Theta}}{2\varepsilon_N^2}\mathbf{s}-\tilde{\mathbf{c}}_m^T\left(\frac{\boldsymbol{\Theta}\left\|\mathbf{s}\right\|^2}{2\varepsilon_N^2}-\boldsymbol{\upsilon}\hat{\mathbf{c}}_m\right)\\&\leq-N(\mathbf{s})(\gamma_1\left\|\mathbf{s}\right\|^{2+2\sigma_2}+\gamma_2\left\|\mathbf{s}\right\|^{2\lambda_2}+\gamma_3\left\|\mathbf{s}\right\|^2)+\mathbf{c}_d^T\boldsymbol{\theta}\left\|\mathbf{s}\right\|-\frac{\mathbf{c}_m^T\boldsymbol{\Theta}}{2\varepsilon_N^2}\left\|\mathbf{s}\right\|^2+\tilde{\mathbf{c}}_m^T\boldsymbol{\upsilon}\hat{\mathbf{c}}_m\end{aligned}\tag{26}$$

According to the Young's inequality, for $\forall\lambda_i>\frac{1}{2},i=(1,2,3)$, the following inequalities can be obtained:

$$\mathbf{c}_d^T\boldsymbol{\theta}\left\|\mathbf{s}\right\|\leq\frac{\mathbf{c}_m^T\boldsymbol{\Theta}}{2\varepsilon_N^2}\left\|\mathbf{s}\right\|^2+\frac{1}{2}\varepsilon_N^2\tag{27}$$

$$\tilde{\mathbf{c}}_m^T\boldsymbol{\upsilon}\hat{\mathbf{c}}_m=\sum_{i=1}^3\upsilon_i\tilde{c}_{mi}\left(c_{mi}-\tilde{c}_{mi}\right)\leq\sum_{i=1}^3\upsilon_i\left(\frac{\lambda_i}{2}c_m^2-\frac{2\lambda_i-1}{2\lambda_i}\tilde{c}_m^2\right)\tag{28}$$

Using the above inequalities, Eq. (26) can be rewritten as

$$
\begin{aligned}
\dot{V}_2 &\le -N(\mathbf{s})(\gamma_1\|\mathbf{s}\|^{2+2\sigma_2}+\gamma_2\|\mathbf{s}\|^{2\lambda_2}+\gamma_3\|\mathbf{s}\|^2)+\frac{1}{2}\varepsilon_N^2+\sum_{i=1}^{3}\left(\upsilon_i\frac{\lambda_i}{2}c_{mi}^2\right)-\sum_{i=1}^{3}\left(\upsilon_i\frac{2\lambda_i-1}{2\lambda_i}\tilde{c}_{mi}^2\right)\\
&\le -N(\mathbf{s})\gamma_1 2^{1+\sigma_2}(\frac{1}{2}\mathbf{s}^T\mathbf{s})^{1+\sigma_2}-N(\mathbf{s})\gamma_2 2^{\lambda_2}(\frac{1}{2}\mathbf{s}^T\mathbf{s})^{\lambda_2}-\sum_{i=1}^{3}\left(\frac{\chi_i}{2\eta_i}\tilde{c}_{mi}^2\right)^{1+\sigma_2}-\sum_{i=1}^{3}\left(\frac{\chi_i}{2\eta_i}\tilde{c}_{mi}^2\right)^{\lambda_2}+\Delta_1
\end{aligned}
\tag{29}
$$

where $\Delta_1=\sum_{i=1}^{3}\left(\frac{\chi_i}{2\eta_i}\tilde{c}_{mi}^2\right)^{1+\sigma_2}+\sum_{i=1}^{3}\left(\frac{\chi_i}{2\eta_i}\tilde{c}_{mi}^2\right)^{\lambda_2}+\sum_{i=1}^{3}\left(\frac{\upsilon_i\lambda_i}{2}c_{mi}^2\right)-\sum_{i=1}^{3}\left(\frac{\chi_i}{\eta_i}\tilde{c}_{mi}^2\right)+\frac{1}{2}\varepsilon_N^2$, $\chi_i=\eta_i\upsilon_i\frac{2\lambda_i-1}{2\lambda_i}$.

If $\frac{\chi_i}{2\eta_i}\tilde{c}_{mi}^2\ge 1$, it has

$$
\left(\frac{\chi_i}{2\eta_i}\tilde{c}_{mi}^2\right)^{1+\sigma_2}+\left(\frac{\chi_i}{2\eta_i}\tilde{c}_{mi}^2\right)^{\lambda_2}-\left(\frac{\chi_i}{\eta_i}\tilde{c}_{mi}^2\right)\le 2\left\{\left(\frac{\chi_i}{2\eta_i}\tilde{c}_{mi}^2\right)^{1+\sigma_2}-1\right\}
\tag{30}
$$

For $\frac{\chi_i}{2\eta_i}\tilde{c}_{mi}^2<1$, it follows that

$$
\left(\frac{\chi_i}{2\eta_i}\tilde{c}_{mi}^2\right)^{1+\sigma_2}+\left(\frac{\chi_i}{2\eta_i}\tilde{c}_{mi}^2\right)^{\lambda_2}-\left(\frac{\chi_i}{\eta_i}\tilde{c}_{mi}^2\right)\le 2\left\{\left(\frac{\chi_i}{2\eta_i}\tilde{c}_{mi}^2\right)^{\lambda_2}-\left(\frac{\chi_i}{2\eta_i}\tilde{c}_{mi}^2\right)\right\}\le 2
\tag{31}
$$

Since $\mathbf{s}$ and $\tilde{\mathbf{c}}_m$ are uniformly bounded, it is assumed that $\tilde{c}_{mi}$ is bounded satisfying $|\tilde{c}_{mi}|<\psi_i$ with positive constants ψ_i, $i=1,2,3$. Then it yields

$$
\left(\frac{\chi_i}{2\eta_i}\tilde{c}_{mi}^2\right)^{1+\sigma_2}+\left(\frac{\chi_i}{2\eta_i}\tilde{c}_{mi}^2\right)^{\lambda_2}-\left(\frac{\chi_i}{\eta_i}\tilde{c}_{mi}^2\right)\le \max\left\{\frac{1}{2^{\sigma_2}}\left(\frac{\chi_i}{\eta_i}\psi_i^2\right)^{1+\sigma_2}-2,2\right\}
\tag{32}
$$

The inequality (29) can be simplified as

$$
\begin{aligned}
\dot{V}_2 &\le -\gamma_1(\frac{1}{2}\mathbf{s}^T\mathbf{s})^{1+\sigma_2}-\sum_{i=1}^{3}\left(\frac{\chi_i}{2\eta_i}\tilde{c}_{mi}^2\right)^{1+\sigma_2}-\gamma_2(\frac{1}{2}\mathbf{s}^T\mathbf{s})^{\lambda_2}-\sum_{i=1}^{3}\left(\frac{\chi_i}{2\eta_i}\tilde{c}_{mi}^2\right)^{\lambda_2}+\Delta_1\\
&\le -\rho_1 V_2^{1+\sigma_2}-\rho_2 V_2^{\lambda_2}+\Delta_2
\end{aligned}
\tag{33}
$$

where $\Delta_2=\sum_{i=1}^{3}\left(\max\left\{\frac{1}{2^{\sigma_2}}\left(\frac{\chi_i}{\eta_i}\psi_i^2\right)^{1+\sigma_2}-2,2\right\}+\frac{\upsilon_i\lambda_i}{2}c_{mi}^2\right)+\frac{1}{2}\varepsilon_N^2$, $\rho_1=\min\left\{\gamma_1,\chi_i^{1+\sigma_2}\right\}$ and $\rho_2=\min\left\{\gamma_2,\chi_i^{\lambda_2}\right\}$.

By **Theorem 1**, it can be concluded that the NFSMS (7) can converge to the $\Omega_1=\left\{\mathbf{s}\,\middle|\,\|\mathbf{s}\|\le\psi_s\right\}$ in a bounded time under the proposed control law. Next, the fixed-time convergence of $\mathbf{e}_1$ and $\mathbf{e}_2$ is analysed from the following three cases.

Case 1: When $\mathbf{s}=\bar{\mathbf{s}}=\mathbf{0}$ is reached, $\mathbf{e}_1$ and $\mathbf{e}_2$ satisfy the following equation

$$
\mathbf{e}_2=-N(\mathbf{e}_1)\left(k_a\mathbf{S}_c+k_b\mathbf{S}_z\right)=-N(\mathbf{e}_1)(k_a\mathbf{sig}^{1+2\sigma_1}(\mathbf{e}_1)+k_b\mathbf{sig}^{2\lambda_1-1}(\mathbf{e}_1))
\tag{34}
$$

Define a Lyapunov function candidate $V_1=\frac{1}{2}\mathbf{e}_1^T\mathbf{e}_1$, its time derivative yields

$$
\begin{aligned}
\dot{V}_1 &= -N(\mathbf{e}_1)\mathbf{e}_1(k_a\mathbf{sig}^{1+2\sigma_1}(\mathbf{e}_1)+k_b\mathbf{sig}^{2\lambda_1-1}(\mathbf{e}_1))\\
&= -N(\mathbf{e}_1)(k_a V_1^{1+\sigma_1}+k_b V_1^{\lambda_1})
\end{aligned}
\tag{35}
$$

Invoking **Theorem 1**, the system states $(\mathbf{e}_1, \mathbf{e}_2)$ are proved to converge to the origin within a fixed time along the NFSMS.

Case 2: When s_i reaches the region Ω_1, for any $|e_{1i}| < \delta$ we have

$$s_i = e_{2i} + N(e_1)\left\{k_a(l_1 e_{1i} + l_2 e_{1i}^2 \operatorname{sgn}(e_{1i}) + l_3 e_{1i}{}^3) + k_b(g_1 e_{1i} + g_2 e_{1i}^2 \operatorname{sgn}(e_{1i}) + g_3 e_{1i}{}^3)\right\} = \psi_{si} \tag{36}$$

where $|s_i| \le \psi_{si}$. Then, $|e_{2i}| < \psi_{si} + N(e_1)\{(k_a l_1 + k_b g_1)\delta + (k_a l_2 + k_b g_2)\delta^2 + (k_a l_3 + k_b g_3)\delta^3\}$

Case 3: When s_i reaches the region Ω_1, for any $|e_{1i}| \ge \delta$ it can be got that

$$e_{2i} + N(e_1)\left\{k_a \operatorname{sig}^{1+2\sigma_1}(e_{1i}) + k_b \operatorname{sig}^{2\lambda_1 - 1}(e_{1i})\right\} = \psi_{si} \tag{37}$$

which can be rewritten as

$$e_{2i} + N(e_1)\left\{\left(k_a - \frac{\psi_{si}}{\operatorname{sig}^{1+2\sigma_1}(e_{1i})}\right)\operatorname{sig}^{1+2\sigma_1}(e_{1i}) + k_b \operatorname{sig}^{2\lambda_1 - 1}(e_{1i})\right\} = 0 \tag{38}$$

$$e_{2i} + N(e_1)\left\{k_a \operatorname{sig}^{1+2\sigma_1}(e_{1i}) + \left(k_b - \frac{\psi_{si}}{\operatorname{sig}^{2\lambda_1 - 1}(e_{1i})}\right)\operatorname{sig}^{2\lambda_1 - 1}(e_{1i})\right\} = 0 \tag{39}$$

Choose k_a, k_b such that $k_a - \frac{\psi_{si}}{\operatorname{sig}^{1+2\sigma_1}(e_{1i})} > 0$ or $k_b - \frac{\psi_{si}}{\operatorname{sig}^{2\lambda_1 - 1}(e_{1i})} > 0$, then it is concluded from **Theorem 1** that e_{2i} will converges to origin in fixed-time. Then, solving (37) leads to $|e_{1i}| \le \psi_{e1}$ after fixed time.

4. SIMULATION RESULTS

A numerical example is provided to demonstrate the effectiveness of our suggested control method in this section. The simulation studies are performed on a SM system with same detail physical parameters and initial conditions are in[13]. The control parameters are set as $k_a = 0.8$, $k_b = 0.6$, $s_m = 0.5$, $s_n = 0.5$, $s_r = 1$, $\delta = 0.001$, $\alpha_1 = 9/7$, $\beta_1 = 15/17$, $\alpha_2 = 9/7$, $\beta_2 = 15/17$, $\gamma_1 = 0.8$, $\gamma_2 = 0.6$, $\gamma_3 = 0.4$, $ss_m = 0.5$, $ss_n = 1.2$, $ss_r = 2$, $\eta_2 = 0.3$, $\eta_1 = 0.8$, $\eta_3 = 2$, $\varepsilon_N = 0.1$, $\upsilon_1 = 0.01$, $\upsilon_2 = 0.01$, $\upsilon_3 = 0.01$.

Figs 1 and 2 show the time-varying curves of the position and velocity trajectory tracking errors, respectively. Obviously, the joint position and velocity trajectories are able to track the desired trajectories within 1s. More specifically, the position tracking error can achieve stable at 0.793s, and the velocity tracking error can achieve stable at 0.912s. Figure 3 gives the time-varying process of control input. As shown in Fig.3, the required input torque is large at the beginning in order to obtain a fast transient response and reaches stability after 1s. In addition, the input torque is chattering free, smooth, and continuous, and. Fig.4 illustrates the estimated parameters of the upper bound of lumped disturbance. As can be observed, all the estimated parameters perform satisfactorily in terms of convergence performance. To this end, the proposed fast fixed-time sliding mode control scheme successfully solves the fixed-time trajectory tracking issue for SM with unknown disturbances and uncertainties. With the suggested control law, tracking performance can be brought to a satisfactory level.

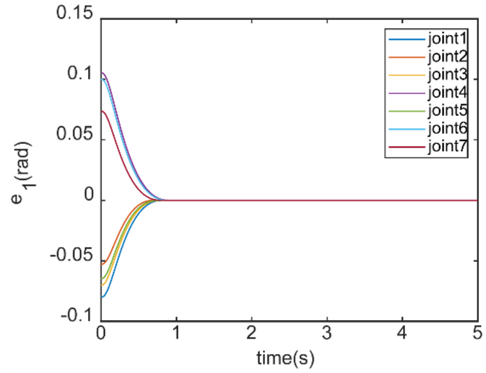

Figure 1. Time-varying of position tracking error

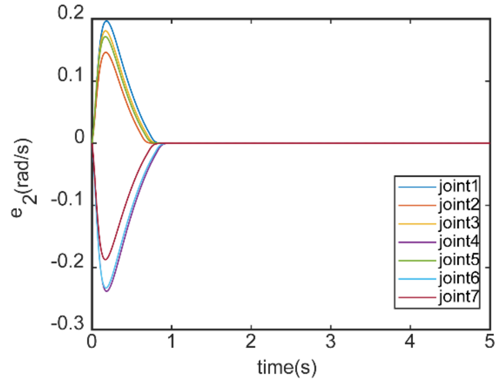

Figure 2. Time-varying of velocity tracking error

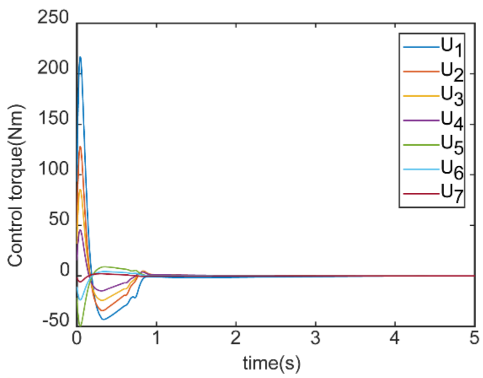

Figure 3. Time-varying of input torque

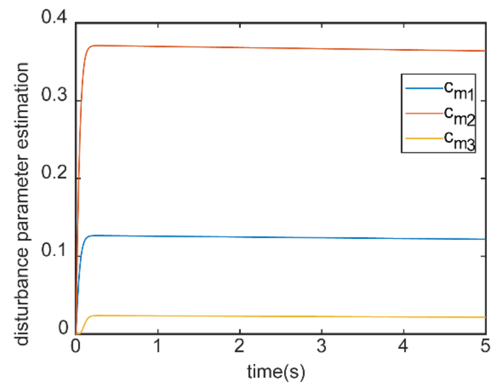

Figure 4. Time-varying of parameter estimation

To further evaluate the fixed-time convergence capability of the suggested controller, four different beginning states are conducted for the SM. Four initial conditions are selected in the simulation as follows:

Case 1: $\mathbf{q}(0) = [0, 1.0472, 0, 0.7854, 0.7854, 0, 0.5236]^T$ rad, $\dot{\mathbf{q}}(0) = [0, 0, 0, 0, 0, 0, 0]^T$ rad/s

Case 2: $\mathbf{q}(0) = [0.02, 0.98, 0.02, 0.8, 0.75, 0.02, 0.55]^T$ rad, $\dot{\mathbf{q}}(0) = [0, 0, 0, 0, 0, 0, 0]^T$ rad/s

Case 3: $\mathbf{q}(0) = [0, \pi/3, 0, \pi/4, \pi/4, 0, \pi/6]^T$ rad, $\dot{\mathbf{q}}(0) = [0.1, 0.2, -0.1, 0.05, 0, 0.05, -0.1]^T$ rad/s

Case 4: $\mathbf{q}(0) = [0.01, 1.01, -0.01, 0.7, 0.8, 0.02, 0.6]^T$ rad, $\dot{\mathbf{q}}(0) = [0.1, 0.2, -0.1, 0.05, 0, 0.05, -0.1]^T$ rad/s

The comparison results of trajectory tracking for four different initial conditions are given in Figs. 5 and 6, respectively. As depicted, the proposed controllers always complete the trajectory tracking tasks in almost the same time and always less than 1s, although under different initial conditions. This implies that the suggested control strategy has the fixed convergence capability with the bounded stabilization time independent of the initial conditions.

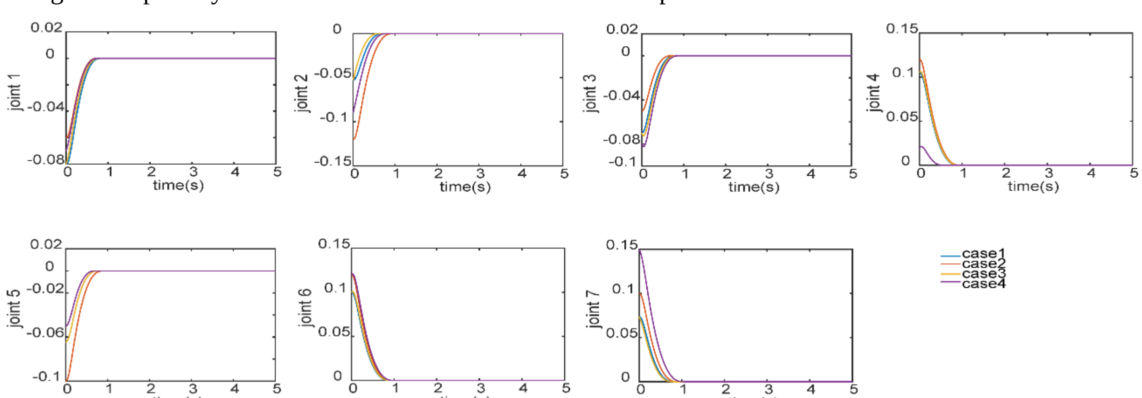

Figure 5. Time-varying of position tracking error under four cases

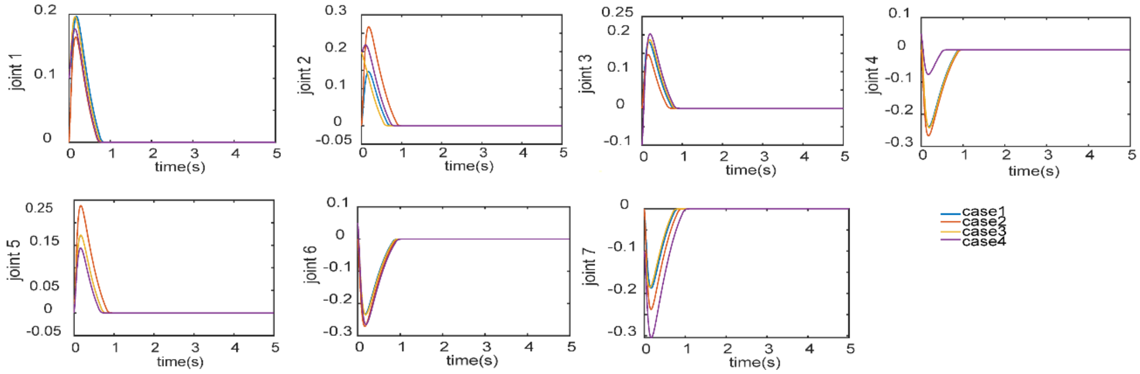

Figure 6. Time-varying of velocity tracking error under four cases

5. CONCLUSION

In this study, a novel fast fixed-time trajectory tracking controller was developed for space manipulator. Despite in spite of unknown disturbances and uncertainties, trajectory tracking manoeuvring was completed after a fixed convergence time for any initial system states. With the proposed scheme, the tracking errors of position and velocity can converge to a small region of the origin within a fixed time. A numerical illustration was provided to demonstrate the validity of the suggested control strategy.

REFERENCES

[1] Flores-Abad, A., Ma, O. and Pham, K., "A review of space robotics technologies for on-orbit servicing," Progress in Aerospace Sciences, 68(8), 126 (2014).
[2] Jia, Q., Yuan, B. and Chen, G., "Adaptive fuzzy terminal sliding mode control for the free-floating space manipulator with free-swinging joint failure," Chinese Journal of Aeronautics, , 34(9), 21 (2021).
[3] Liu, F., Li, Q. and Liang, L., "Adaptive backstepping sliding mode control of space manipulators' trajectory tracking in different gravity environments," Chinese High Technology Letters, 25(1), 384-392 (2015).
[4] Yao, Q., "Adaptive fuzzy neural network control for a space manipulator in the presence of output constraints and input nonlinearities," Advances in Space Research, 67(6), 1830-1843 (2021).
[5] Jia, S. and Shan, J., "Finite-time trajectory tracking control of space manipulator under actuator saturation," IEEE Transactions on Industrial Electronics, 67(3), 2086-2086 (2020).
[6] Chen, Q., Xie, S. and He, X., "Neural-Network-Based Adaptive Singularity-Free Fixed-Time Attitude Tracking Control for Spacecrafts," IEEE Transactions on Cybernetics, 51(10), 5032-5045 (2021).
[7] Chen, M., Wang, H. and Liu, X., "Adaptive Fuzzy Practical Fixed-Time Tracking Control of Nonlinear Systems," IEEE Transactions on Fuzzy Systems, 29(3), 664-673 (2021).
[8] Jin, R., Rocco, P. and Geng, Y., "Observer-based fixed-time tracking control for space robots in task space," Acta Astronautica, 184(6), 35-45 (2021).
[9] Su, Y., Zheng, C. and Mercorelli, P., "Robust approximate fixed-time tracking control for uncertain robot manipulators," Mechanical Systems and Signal Processing, 135(2), 106379 (2020).
[10] Shao, X., Sun, G. and Xue, C., "Nonsingular terminal sliding mode control for free-floating space manipulator with disturbance," Acta Astronautica, 181(2), 396-404 (2021).
[11] Cao, L., Xiao, B. and Golestani, M., "Faster fixed-time control of flexible spacecraft attitude stabilization," IEEE Transactions on Industrial Informatics, 16(2), 1281-1290 (2019).
[12] Li, H., Cai, Y., "Fixed-time non-singular terminal sliding mode control with globally fast convergence," IET control theory & applications, 16(12), 1227-1241 (2022).
[13] Yan, Y.X., Cui, H.T. and Han, P., "Fixed-time control for free-floating space manipulators with prescribed constraints and input saturation," The Aeronautical Journal, 12(3), 1-26 (2023).